

NOVEL CARBON ADSORBENTS FOR FUEL GAS STORAGE DERIVED FROM LIGNOSULFONATE WASTE

Emmanuelle Alain¹, Brian McEnaney¹, Oleksandr Kozynchenko^{2,3}, and Vladimir Strelko²

¹ Materials Research Centre, Department of Engineering and Applied Science, University of Bath, Bath, BA2 7AY, United Kingdom.

² National Academy of Sciences, Institute of Sorption and Problems of Endoecology, Kiev, Ukraine.

³ MAST Carbon Ltd, Henley Park, Guilford, GU3 2AF, United Kingdom

KEYWORDS carbon adsorbents, fuel gas, lignosulfonate waste

INTRODUCTION

There has been a resurgence of interest in using adsorbent carbons for fuel gas storage (natural gas and hydrogen). Molecular simulations of adsorption at ambient temperatures of methane (as a model for natural gas) [1] in slit-shaped carbon pores indicate an optimal micropore width for methane storage of ~11 Å. Thus, to optimise the storage capacity requires maximisation of micropore volume, of about this width, and minimisation of mesoporosity, macroporosity and void space between the carbon particles [2]. A storage system for road vehicles powered by natural gas requires a delivered volumetric capacity of ~150 v/v. These requirements have prompted the development of a number of routes for fabrication of highly microporous carbon monoliths with storage capacities that approach or meet the target [e.g., 2-5]. Thus, future work should be aimed towards the development of carbon monoliths by inexpensive and flexible methods. In this paper we report the preparation and characterisation of activated carbon monoliths from lignosulfonate resins derived from waste products in the paper pulp industry.

EXPERIMENTAL

Precursor Materials. Lignin is a high molecular weight, polyphenolic biopolymer and an important constituent of wood (~30 wt% dry basis). Lignosulfonates are waste products of the paper pulp industry formed by treatment of wood with strong alkali solutions saturated with sulphur dioxide. The lignosulfonate used in this study was received as a sodium salt from the Kondopoga plant in the north of European Russia. Spherical lignosulfonate resins were produced by emulsion, polycondensation reactions with cross-linking reagents; the details of the formulations used for the polymerisations are proprietary.

Carbon Microbeads. Spherical resin beads, M1, were carbonised in flowing argon by heating to 900 °C to produce carbon beads, M2. Heating in flowing carbon dioxide at 900 °C for different times produced two activated carbons M3 and M4 with 44 and 55 wt% burn-off respectively. A third activated carbon bead sample (59 wt % burn-off), L5, was made in the same way, but starting from a resin produced from a different polymerisation formulation.

Resin and Carbon Discs. The resin microbeads were pressed into resin discs (4.0 x 0.1 cm), A-1, at 100 °C and 3.2 kN cm⁻². Carbon discs, A-3, were prepared from A-1 by carbonisation in CO₂ at 600 °C for 1.5 h. An activated carbon disc, D-4, was prepared by addition of the activation catalyst potassium acetate (2 wt% K⁺) to resin microbeads prior to pressing into discs. The discs were then carbonised/activated by heating to 600 °C for 1.5 h. The burn-off of the activated carbon discs was estimated as 25-30%. The various routes for the production of carbons from the resin microbeads are summarised in Figure 1.

Characterisation Methods. The general morphology of the bead and disc samples was studied using SEM (JEOL 6310). Samples were spread on a graphite pad and gold sputtered. The packing density of the bead samples and piece (bulk) densities of the disc samples were measured using standard methods. Surface areas and micropore volumes were determined from N₂ adsorption at 77 K (Micromeritics ASAP 2010). Methane adsorption at 298 K and up to 8 bar was measured gravimetrically using a Hidden Intelligent Gravimetric Analyser.

RESULTS AND DISCUSSIONS

Microscopy. The spherical resin, M1, Figure 2(a), consists mainly of agglomerated spheres with a wide range of diameters (70-800 µm); only the largest microbeads are isolated. The extent of agglomeration in the carbon spheres, M2, and the activated spherical carbon, M3, M4, is much reduced and many more isolated particles are found, Figure 2(b)-(c). There is evidence for preferential attack at former points of contact in the case of the activated carbon

beads and broken particles reveal that some are solid spheres while others have hollow centres (shells). The same observations apply to the L5 sample. A comparison of the resin disc A-1, the carbon disc A-3 and the activated carbon disc D-4, Figure 3, illustrates the volumetric shrinkage (~67%) that occurs upon carbonisation. SEM of the discs, Figure 2 (d), shows that the pressing process leads to agglomeration of the resin microbeads and in some areas of the discs there is a transformation to a continuous structure.

Nitrogen Isotherms. Adsorption of nitrogen at 77 K on the carbon microbeads M2, Figure 4(a), and the activated carbons M3 and M4 indicate qualitatively that the carbons are microporous. For the activated carbons there is hysteresis at high relative pressures ($P/P_0 > 0.8$) that is type H1 in the IUPAC classification [6]. This is attributed to condensation in the interstices between the carbon spheres. The isotherm of the carbon material L5, Figure 4(b) shows hysteresis of type H3 that is indicative of a small amount of mesoporosity. This shows that the pore structure of the carbon beads can be controlled to some extent by varying the polymerisation conditions. The nitrogen adsorption isotherms for the carbon discs, A-3 and D-4, at low relative pressure, Figure 4(c), are more rectangular than those for the loose spherical carbons, indicating that they contain narrow micropores. Type H4 hysteresis is seen, indicative of microporosity with a type I isotherm. The gravimetric adsorptive capacities of the carbon discs are clearly less than those of the carbon microbeads, as reflected in the BET surface areas of the carbons, Table 1, and the micropore volumes, V_0 , determined using the Dubinin-Astakhov equation.

Methane Adsorption. Gravimetric isotherms for adsorption of methane at 298 K on activated carbons M4 and L5 and activated carbon disc D-4 are in Figure 5. It is notable that the gravimetric methane uptake by the activated carbon disc D-4 up to ~4 bar is comparable to the uptake by the activated carbon beads M4 and L5. This is in contrast to nitrogen uptake by these carbons, Figure 4.

The maximum pressure attainable in this study is 8 bar, but the practical target storage pressure for methane is 34 bar. We have shown previously [7] that the gravimetric capacity at 34 bar, $n(P)$, can be estimated accurately by extrapolation from the lower pressure data using the Tóth adsorption isotherm equation [8]:

$$n(P) = \left(\frac{mP}{b + P^t} \right)^{1/t} \quad (1)$$

where m , b and t are parameters of the equation obtained by curve fitting. Estimates of $n(P)$ at 34 bar and measured values for 1 bar for the activated carbon microbeads M4 and L5 and the activated carbon disc D-4 are given in Table 2. As indicated in Figure 5, the gravimetric capacity, $n(P)$, for the activated carbon discs D-4 at 34 bar is lower than those for the activated carbon spheres M4 and L5, but the reverse is true at 1 bar. This is another indication that the carbon discs have narrower micropores than do the carbon microbeads.

Volumetric Methane Capacities. The key criterion for evaluating the suitability of activated carbons for natural gas storage is the volumetric capacity expressed as volume of methane at 298 K per volume of activated carbon, including inter-particle voids. Three methane capacities can be taken into account: the adsorbed, the stored and the delivered capacities. The *adsorbed capacity*, V_a , is defined as the excess volume of methane adsorbed in micropores per volume of activated carbon. The adsorption isotherm expressed as gravimetric methane uptake, $n(P)/\text{mmol g}^{-1}$ vs. P is an excess isotherm which measures the excess methane adsorbed in pores, excluding methane stored in the gas phase. It is given by

$$V_a = 24.465 n(P) \rho_a \quad (2)$$

where ρ_a is the packing density for powders or the bulk (piece) density for monoliths. The *stored capacity*, V_s , is defined as the sum of methane stored in the adsorbed phase, V_a , and in the gas phase, V_g , at pressure, P , (3.4 MPa, 34 bar) where

$$V_g = \frac{PV_t \rho_a}{zP_0} \sim 36V_t \rho_a \quad (3)$$

and z is the compressibility of methane at P ($= 0.93$ at 34 MPa and 298 K), P_0 is a reference pressure (1 bar) and V_t , the total pore volume, including micropores, mesopores, macropores and inter-particle voids.

$$V_t = (1 - \frac{\rho_s}{\rho_c}) \sim (1 - 0.5 \rho_a) \quad (4)$$

where ρ_c is the skeletal density of solid carbon ($\rho_c \sim 2.0 \text{ g cm}^{-3}$). There is an uncertainty on whether or not the micropore volume should be included in the calculation of compressed methane gas in pores. If the micropores are fully occupied by adsorbed gas, then they should be

excluded from the calculation. In reality, the stored methane capacity should lie between the two extreme values:

$$V_s = V_a + 36(1 - 0.5\rho_a) \quad (5) \text{ (a) (b)}$$

$$V_s = V_a + 36(1 - 0.5\rho_a - V_0\rho_a)$$

The delivered capacity, V_d , is simply the difference between the stored capacity at the storage pressure (3.4MPa, 34 bar) and the stored capacity at the release pressure (0.1 MPa, 1 bar)

$$V_d = V_s(3.4\text{MPa}) - V_s(0.1\text{MPa}) \quad (6)$$

Table 2 shows that although the activated carbon beads M4 have the highest gravimetric methane capacity, the activated carbon disc has the highest stored and delivered capacity. Here, the lower gravimetric capacity of the discs is offset by their higher bulk density. By contrast, the delivered volumetric methane capacities of the carbon microbeads are modest due to the high volume fraction of inter-particle voids. The delivered capacities found for the activated carbon discs, D-4, approach the target value of 150 v/v. It is likely that this target can be achieved with further refinement of the microstructure of the carbons. For example the value of V_a (≈ 36 v/v) found for the discs D-4 at 1 bar is almost twice the values found for the loose activated carbon spheres. This is another reflection of the presence of narrow micropores in the carbon discs. The amount of methane retained in the discs at 1 bar can be reduced if the micropore size distribution can be widened slightly.

CONCLUSIONS

Porous spherical resins of different particle sizes can be produced by emulsion polycondensation of lignosulfonates with cross linking agents. These resin can be converted directly into activated carbon beads or pressed into discs that can be converted into activated carbon monoliths. The delivered volumetric capacities of the loose activated carbons are modest (~ 81 - 112 v/v) due to the high volume fraction of inter-particle voids. The delivered capacity of the activated carbon discs approach the target capacity of 150 v/v. The flexibility of the fabrication route for producing carbons from lignosulfonate resins suggests that this target can be reached with further development.

ACKNOWLEDGEMENT. We acknowledge financial support from the EU INTAS programme, Contract 96-1023 and EU TMR programme, Contract ERBFMBICT972773.

REFERENCES

1. Matranga, K.R., Myers, A.L. and Glandt, E.D., *Chem. Eng. Sci.*, **47** (1992) 1569
2. Chen, X.S., McEnaney, B., Mays, T.J., Alcaniz-Monge, J., Cazorla-Amoros, D. and Linares-Solano, A., *Carbon*, **35** (1997) 1251
3. Quinn, D.F. and MacDonald, J.A., *Carbon*, **30** (1992) 1097
4. Bose, T., Chahine, R. and Arnaud, J.M., *US Patent 4999330* (1991)
5. Manzi, S., Valladares, D., Marchese, J. and Zgrablich, G., *Adsorption. Sci. Tech.*, **15** (1997) 301
6. Gregg, S.J. and Sing, K.S.W., in *Adsorption, Surface Area and Porosity*, London, Academic Press (1982)
7. Alain, E., McEnaney, B., Mays, T.J., Strelko, V. and Kozynchenko, O., *Extended Abstracts 'Carbon '99'*, American Carbon Society, Charleston, SC, USA, (1999) 784
8. Valenzuela, D.P. and Myers, A.L., in *Adsorption equilibrium data handbook*, Prentice Hall, Englewood Cliffs, (1989) 8

Table 1. Particle bulk densities, ρ_a , BET surface areas, S_{BET} , and D-A micropore volumes, V_0 for activated lignosulfonate carbons.

Material	$\rho_a / (\text{g cm}^{-3})$	$S_{BET} / (\text{m}^2 \text{g}^{-1})$	$V_0 / (\text{cm}^3 \text{g}^{-1})$
Spherical activated carbons, M3	0.37	1202	0.64
Spherical activated carbons, M4	0.33	1610	0.92
Spherical activated carbons, L5	0.47	1235	0.58
Activated carbon discs, A-3	1.26	335	0.17
Activated carbon discs, D-4	0.95	676	0.33

Table 2. Methane capacities at 298 K for activated lignosulfonate carbon beads and discs.

Material	$n(P) / (\text{mmol g}^{-1})$ 34 & 1 bar ^b	V_a 34 & 1 bar ^b	V_s 34 bar ^c	V_d^c
Spherical activated carbons M4 (1) ^a	9.5 & 1.4	77 & 11	96~107	85~96
Spherical activated carbons M4 (2) ^a	9.1 & 1.4	73 & 11	92~103	81~92
Spherical activated carbons L5 (1) ^a	8.6 & 1.3	99 & 15	117~126	102~111
Spherical activated carbons L5 (2) ^a	8.7 & 1.3	100 & 15	118~127	103~112
Activated carbon discs D-4	6.5 & 1.6	152 & 36	159~170	123~134

a. Duplicate samples.

b. Values at 34 bar estimated using the Tóth equation, measured values at 1 bar.

c. Higher and lower values calculated using Equation 5 (a) and 5 (b) resp.

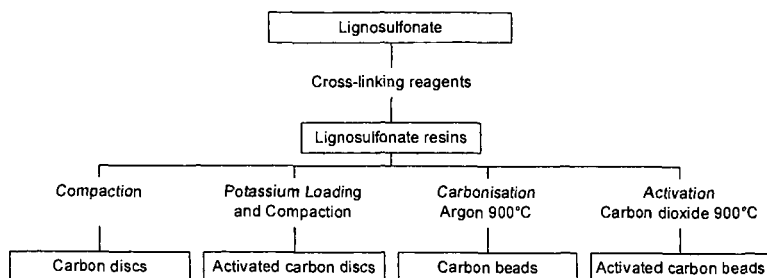


Figure 1. Flow diagram for production of the carbons derived from lignosulfonate resins.

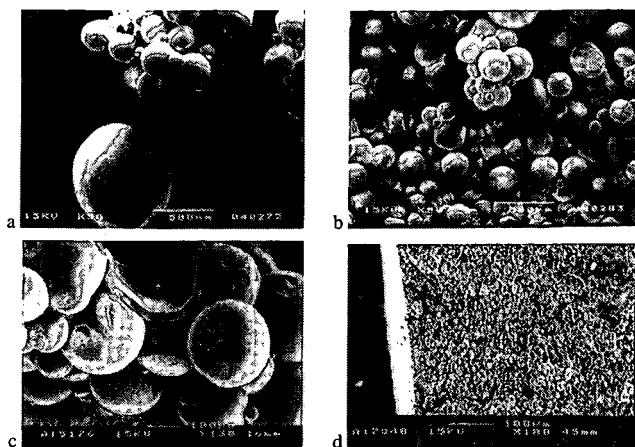


Figure 2 (a)-(d). SEM micrographs of the carbons

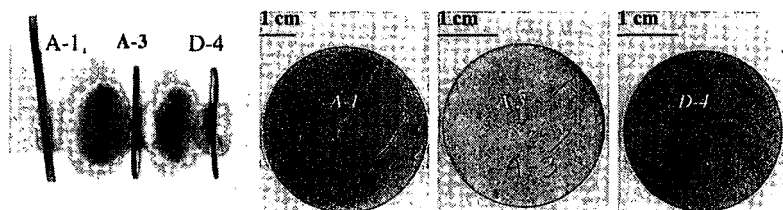


Figure 3. Optical macrographs of the discs

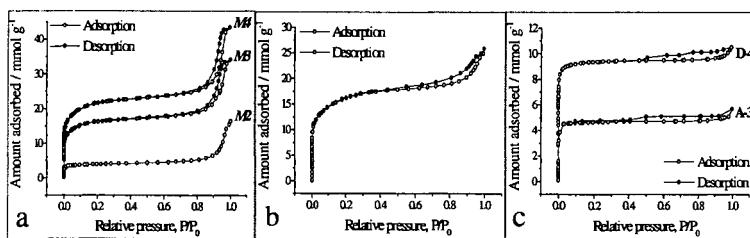


Figure 4. Nitrogen adsorption isotherms (a) M2-M4; (b) L5; (c) A-3, D-4.

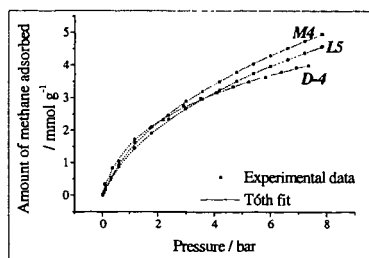


Figure 5. Measured methane isotherms at 298K and their Tóth fits.